Unified continuum approach to crystal surface morphological relaxation

Dionisios Margetis

*Department of Mathematics and Institute for Physical Science and Technology, University of Maryland,
College Park, Maryland 20742, USA*

A continuum theory is used to predict scaling laws for the morphological relaxation of crystal surfaces in two independent space dimensions. Our goal is to unify previously disconnected experimental observations of decaying surface profiles. The continuum description is derived from the motion of interacting atomic steps. For isotropic diffusion of adatoms across each terrace, induced adatom fluxes transverse and parallel to step edges obey different laws, yielding a *tensor* mobility for the continuum surface flux. The partial differential equation for the height profile expresses an interplay of step energetics and kinetics, and aspect ratio of surface topography that plausibly unifies observations of decaying bidirectional surface corrugations.

Novel small devices rely on the stability of nanoscale surface features. The lifetimes of nanostructures decaying via surface diffusion scale as a large power of their size and increase with decreasing temperature. Below roughening, crystal surfaces evolve via the motion of atomic steps bounding nanoscale terraces.[1,2]

Experiments with decaying surface features[3–6] are useful for testing step models. Particularly informative are observations of bidirectional corrugations relaxing below roughening.[3–6] In lithography-based experiments,[3] where initial wavelengths in two directions differ significantly and profiles depend nearly on one space dimension (1D), the surface height decays exponentially with time. By contrast, in sputter-rippling experiments,[5,6] where initial wavelength ratios are closer to unity and profiles evidently depend on two space dimensions (2D), height spatial-frequency components decay inversely linearly with time. These observations have previously evaded a unified theory.[7,8] In this Brief Report, we use a continuum theory to plausibly unify these observations via an appropriate *tensor mobility*.

There are two main theoretical approaches to crystal surface morphological evolution below roughening. One approach follows the motion of steps in the spirit of the Burton-Cabrera-Frank model[1] via numerical solutions of coupled equations for step positions.[9,10] Step simulations in one dimension[9] show exponential decay of surface corrugations with attachment-detachment limited (ADL) kinetics, in agreement with lithography experiments.[3] Step simulations in 2D invoke axisymmetry[10] and are thus limited in their ability to make predictions for general surface morphologies.

Another approach relies on equilibrium thermodynamics and mass conservation using continuum evolution laws[11–14] such as partial differential equations (PDEs), which enable simple scaling predictions.[12] Continuum models are criticized for their inaccurate description of macroscopic, planar surface regions ("facets"),[9] but progress is made in including facets in evolution laws.[15] Continuum theories have not previously unified observations of decaying surface corrugations.[8] An ingredient of such theories is the *scalar* mobility for the adatom flux in 2D,[7,12–14] which does not distinguish adatom fluxes parallel to steps from fluxes transverse to steps. This formulation is valid when steps are ev-

erywhere parallel[12] but is shown here to be inadequate in general cases.

In this Brief Report, we plausibly unify experimental observations of decaying profiles by invoking a *tensor macroscopic mobility* for adatom fluxes that stem from *isotropic* terrace diffusion; see Eqs. (8)–(10). An elaborate derivation is given in Ref. 16. Here, we provide a more general yet simpler derivation. A discrete version of this mobility is found in Ref. 17. We show that the resulting PDE for the height reduces to known evolution laws for one-dimensional geometries; also, we relate scaling predictions of the PDE to relaxation experiments. We find that observed decay laws with time can arise from competition of step kinetics and surface topography. This effect is due to coupling of flux components via terrace diffusion and is distinct from the influence of step-edge diffusion; see, e.g., Ref. 18. The similar effect of anisotropic terrace diffusion on step meandering is studied in Ref. 19. By contrast to Ref. 19, our model has scalar microscopic parameters.

First, we describe the step flow model.[1] A top terrace is surrounded by non-self-intersecting and noncrossing steps numbered $i = 1, 2, \ldots$; $i = 1$ denotes the top step. The projection of steps on the basal plane is described by the vector $\mathbf{r}(\eta, \sigma, t)$; t is time, $\eta = \eta_i$ at the ith step, $\eta_i < \eta < \eta_{i+1}$ on the ith terrace, and σ is the position along each step (see Fig. 1). The unit vectors normal and parallel to steps in the direction of increasing η and σ are $\mathbf{e}_\eta$ and $\mathbf{e}_\sigma$; $\mathbf{e}_\eta \cdot \mathbf{e}_\sigma = 0$. The metric coefficients (to be used below) are $\xi_\eta = |\partial_\eta \mathbf{r}|$ and $\xi_\sigma = |\partial_\sigma \mathbf{r}|$; $\partial_\eta := \partial/\partial\eta$.

Mass conservation for atoms is described by

$$v_i = \mathbf{e}_\eta \cdot \left. \frac{d\mathbf{r}}{dt}\right|_{\eta=\eta_i} = \frac{\Omega}{a}[J_{i-1}^\eta(\eta_i, \sigma, t) - J_i^\eta(\eta_i, \sigma, t)]. \quad (1)$$

v_i is the (normal) velocity of the ith step; Ω is the atomic volume; a is the step height; $J_i^\eta = \mathbf{J}_i \cdot \mathbf{e}_\eta$ is the adatom flux (adatoms/length/time) normal to steps; $\mathbf{J}_i = -D_s \nabla C_i$ is the (vector) flux on the ith terrace; D_s is the terrace diffusivity, a scalar; and $C_i(\mathbf{r}, t)$ is the adatom density [adatoms/(length)²] on the ith terrace. In the quasistatic approximation, C_i solves the diffusion equation $\nabla^2 C_i \approx 0$, where no material is deposited from above. The boundary conditions for atom
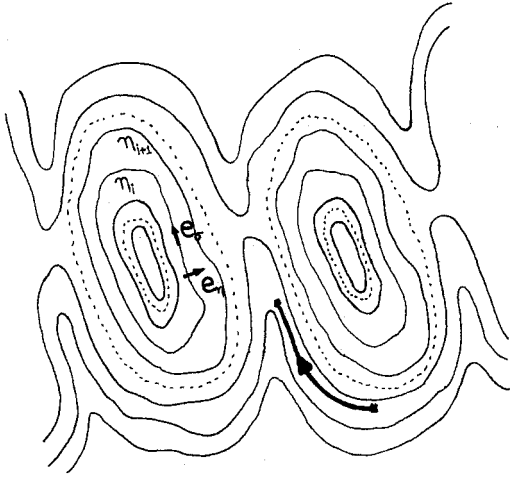
FIG. 1. Schematic of steps on the basal plane. Local coordinates relative to a top terrace are (η, σ). The arrow shows longitudinal flux directed to a valley. Dots denote many steps.

attachment-detachment at the ith and $(i+1)$th steps are[10]

$$\mp J_i^\eta(\eta_l, \sigma') = k[C_i(\eta_l, \sigma') - C_l^{eq}(\sigma')]. \qquad (2)$$

In Eq. (2), the t dependence is omitted, $l=i$ (upper sign) or $i+1$ (lower sign), k is the attachment-detachment rate, and C_i^{eq} is the ith-step equilibrium atom density. Note that Eq. (2) is similar to those of other growth problems, but here, there is no morphological instability.

Next, we close Eqs. (1) and (2) by relating C_i^{eq} with the step positions. First, we introduce the ith-step chemical potential $\mu_i(\sigma, t)$, the change in the step energy by adding or removing an atom at (η_i, σ) (Ref. [10]): $C_i^{eq} = C_s e^{\mu_i/(k_BT)} \sim C_s(1 + \frac{\mu_i}{k_BT})$, where $|\mu_i| \ll k_BT$, C_s is the atom equilibrium density near a straight isolated step, and k_BT is Boltzmann's energy.

Second, we provide a relation of μ_i with the step positions. We use $U(\eta, \sigma)$, the energy per length of the ith step; thus, the length $\delta s_i = \xi_\sigma \delta \sigma$ of the ith step has energy $\delta W_i = U(\eta_i, \sigma) \delta s_i$. Addition or removal of atoms at (η_i, σ) changes η_i by $\delta \eta$ assuming energy isotropy; so, the step moves along the local normal ($\mathbf{e}_\eta$) by $\delta \varrho = \xi_\eta \delta \eta$ and the step energy changes by $\delta^2 W_i = [\partial_{\eta_i}(\delta W_i)] \delta \eta$. By definition of μ_i, $\mu_i = \frac{\Omega}{a} \frac{\delta^2 W_i}{\delta \varrho \delta s_i}$ as $(\delta \sigma, \delta \eta) \to 0$, we find

$$\mu_i = (\Omega/a) \left[(\partial_\eta U)\xi_\eta^{-1} + \kappa U(\eta, \sigma)\right]\big|_{\eta = \eta_i}, \qquad (3)$$

where κ is the step curvature and $U = \gamma + U^{int}$; γ is the step line tension, assumed a constant, and U^{int} accounts for interactions with other steps. For nearest-neighbor elastic-dipole or entropic repulsions, U^{int} is[2,20]

$$U^{int} = g\left[\frac{\Phi(\eta, \eta_{i+1}; \sigma)}{(\eta_{i+1} - \eta)^2} + \frac{\Phi(\eta, \eta_{i-1}; \sigma)}{(\eta - \eta_{i-1})^2}\right], \qquad (4)$$

where g (energy/length) is positive and $\Phi(\eta, \zeta; \sigma)$ is geometry dependent, differentiable with (η, ζ) and satisfies $\Phi(\eta_i, \eta_{i+1})\delta s_i = \Phi(\eta_{i+1}, \eta_i)\delta s_{i+1}$.[16] Suppressing η_{i-1} and η_{i+1}, Eqs. (3) and (4) yield $\mu_i = \tilde{\mu}(\eta = \eta_i, \sigma)$.

Equations (1)–(4) describe step motion via adatom isotropic diffusion and atom attachment-detachment at steps. To enable predictions at length scales large compared to the terrace width $\delta \varrho_i$, we next derive a PDE for the continuum height profile $h(\mathbf{r}, t)$. Thus, $\delta \varrho_i$ is much smaller than (i) the length over which the step density $\frac{a}{\delta \varrho_i}$ varies and (ii) the step radius of curvature, $1/\kappa$. We take $\delta \eta_i = \eta_{i+1} - \eta_i \to 0$ with fixed $\frac{a}{\delta \rho_i}$. In this limit, $\frac{a}{\delta \rho_i} \to |\nabla h|$, where $\nabla h = (\partial_x h, \partial_y h)^T$, and $v_i \to \frac{\partial_t h}{|\nabla h|}$.

Firstly, the familiar continuum mass conservation law for atoms comes from the step velocity law, Eq. (1). By using the continuous extension $\mathbf{J}(\mathbf{r})$ of $\mathbf{J}_i(\eta_i, \sigma)$, we have

$$\partial_t h = -\frac{\Omega}{\xi_\sigma \xi_\eta}[\partial_\eta(\xi_\sigma J^\eta) + \partial_\sigma(\xi_\eta J^\sigma)] = -\Omega \nabla \cdot \mathbf{J}. \qquad (5)$$

Next, we apply Eq. (2) to relate $\mathbf{J}(\mathbf{r}, t)$ to the continuum step chemical potential $\mu(\mathbf{r}, t) = \tilde{\mu}(\eta_i, \sigma, t)$. The following procedure is more general than the analysis in Ref. [16]. (i) We apply Eq. (2) with the upper sign for $\sigma' = \sigma$ and with the lower sign for $\sigma' = \sigma + \delta \sigma$. (ii) We expand the transverse current J_i^η, the density C_i, and $\tilde{\mu}$, each evaluated at $(\eta_{i+1}, \sigma + \delta \sigma)$, at (η_i, σ) using $\mathbf{J}_i = -D_s \nabla C_i$, e.g., $C_i\big|_{i+1, \sigma + \delta \sigma} \approx C_i\big|_i - D_s^{-1}(\xi_\eta \delta \eta_i J_i^\eta\big|_i + \xi_\sigma \delta \sigma J_i^\sigma\big|_i)$, where $Q\big|_p := Q(\eta_p, \sigma)$ and $J_i^\sigma = \mathbf{J}_i \cdot \mathbf{e}_\sigma$ is the longitudinal current. (iii) We subtract the $\pm$ parts of Eq. (2) dropping terms that are negligible as $\delta \eta_i \to 0$. Thus, we find

$$\left(1 + q\frac{a}{\delta \rho_i}\right)J^\eta + \frac{C_s D_s}{k_BT}\frac{\partial_\eta \tilde{\mu}}{\xi_\eta} + \frac{\xi_\sigma}{\xi_\eta}\left(J_i^\sigma + \frac{C_s D_s}{k_BT}\frac{\partial_\sigma \tilde{\mu}}{\xi_\sigma}\right)\delta \sigma = 0, \qquad (6)$$

where $q = \frac{2D_s}{ka}$. By setting $\delta \sigma = 0$ in Eq. (6), we obtain

$$J_i^\eta \to \mathbf{J}(\mathbf{r}, t) \cdot \mathbf{e}_\eta = -\frac{D_s C_s}{k_BT}\frac{1}{1 + q|\nabla h|}\frac{\partial_\eta \mu}{\xi_\eta}, \qquad (7a)$$

where $(a/\delta \rho_i)q$ is fixed. Hence, Eq. (6) reduces to

$$J_i^\sigma \to \mathbf{J}(\mathbf{r}, t) \cdot \mathbf{e}_\sigma = -\frac{D_s C_s}{k_BT}\frac{\partial_\sigma \mu}{\xi_\sigma}. \qquad (7b)$$

By Eq. (7b), the longitudinal flux J^σ has the terrace diffusivity D_s, whereas the normal flux J^η, Eq. (7a), has the slope-dependent diffusivity $\tilde{D}_s = D_s(1 + q|\nabla h|)^{-1}$, cf. Ref. [17]. Note that $\tilde{D}_s = D_s$ for terrace diffusion limited (TDL) kinetics, $q|\nabla h| \ll 1$. The distinction between J^σ and J^η results from coarse graining in 2D, which combines atom attachment-detachment, terrace diffusion, and step topography. For ADL kinetics, $q|\nabla h| \gg 1$, J^η depends on *step* variations of μ since steps are sources and sinks of atoms by Eq. (2), whereas J^σ is sensitive to *space* variations of μ along steps due to adatom diffusion between nonparallel steps. Equations (7a) and (7b) read $\mathbf{J} = -C_s \mathbf{M} \cdot \nabla \mu$, where the mobility $\mathbf{M}$ (length^2/energy/time) is a second-rank *tensor*. In the basal's plane Cartesian system (x, y), the matrix elements M_{ij} ($i, j = x, y$) are

$$M_{xx} = \frac{D_s}{k_BT}\frac{(\partial_x h)^2}{|\nabla h|^2}\left[\frac{1}{1 + q|\nabla h|} + \alpha^2\right], \qquad (8)$$

$$M_{xy} = M_{yx} = -\frac{D_s}{k_B T} \frac{q|\nabla h|}{1 + q|\nabla h|} \frac{(\partial_x h)^2}{|\nabla h|^2} \alpha, \tag{9}$$

$$M_{yy} = \frac{D_s}{k_B T} \frac{(\partial_x h)^2}{|\nabla h|^2} \left[\frac{\alpha^2}{1 + q|\nabla h|} + 1 \right], \tag{10}$$

where $\alpha := \frac{\partial_y h}{\partial_x h}$. For biperiodic profiles, α is estimated by $\frac{\lambda_x}{\lambda_y}$, the (aspect) ratio of dominant (maximum-amplitude) wavelengths in x and y; we take $\lambda_x \leq \lambda_y$ and, thus, $\alpha \leq 1$.

Next, we obtain a PDE for the height profile $h(\mathbf{r}, t)$. First, we derive a relation between μ and ∇h via Eqs. (3) and (4) by expanding in $(\eta_i - \zeta)$ the function $\Phi(\eta_i, \zeta; \sigma)$ of Eq. (4), where $\zeta = \eta_{i+1}$ or η_{i-1}.[16] After some algebra, the limit $\delta \eta_i \to 0$ of $\mu_i = \tilde\mu(\eta = \eta_i, \sigma)$ yields

$$\mu = \Omega[g_1 \kappa - g_3 \nabla \cdot (|\nabla h| \nabla h)], \tag{11}$$

where $\kappa = -\nabla \cdot \frac{\nabla h}{|\nabla h|}$ is the step-edge curvature, $g_1 = \frac{\gamma}{a}$, and $g_3 = \frac{3g}{a} \left(\frac{\xi_\eta}{a} \right)^2 \Phi(\eta_i, \eta_i)$; g_1 and g_3 have dimensions of energy per area. This μ also results from the variational derivative of the surface energy $E = \iint dxdy[g_1|\nabla h| + (g_3/3)|\nabla h|^3]$.[11,12,16] By Eqs. (5), (7a), (7b), and (11),

$$\partial_t h = B \nabla \cdot \left\{ \mathbf{\Lambda} \cdot \nabla \left[\nabla \cdot \left(\frac{\nabla h}{|\nabla h|} \right) + \frac{g_3}{g_1} \nabla \cdot (|\nabla h| \nabla h) \right] \right\}, \tag{12}$$

where $\mathbf{\Lambda} = -\frac{k_B T}{D_s} \mathbf{M}$ and $B = \frac{D_s C_s g_1 \Omega^2}{k_B T}$ [(length)^4/time]. By Eqs. (8)–(10) for $\mathbf{M}$, Eq. (12) describes an interplay of step energetics and kinetics, and aspect ratio α. This dependence on α is absent in previous studies of morphological evolution below roughening.[7,12–14]

It is tempting to compare ingredients of Eq. (12) to similar treatments of steps, e.g., Ref. 19 for a step meander without deposition. The last term of Eq. (14) in Ref. 19 pertains to the flux along the step edge, with a mobility that depends on the step-edge slope; in the small-slope limit, this term appears to agree with Eq. (7b). We emphasize that the (isotropic) physics for each terrace in our model is different from that of Ref. 19 where anisotropic terrace diffusion coexists with step-edge diffusion.

We now show that Eq. (12) reduces to known macroscopic laws for everywhere parallel steps. We set $J^\sigma = 0$ by which the effective mobility becomes $M = \frac{D_s}{k_B T}(1 + q|\nabla h|)^{-1}$, a scalar. For straight steps (in 1D), $\eta = x$, we additionally have $\kappa \equiv 0$ and the PDE becomes $\partial_t h = -B_3 \partial_x[(1 + q|\partial_x h|)^{-1} \partial_{xx}(|\partial_x h|\partial_x h)]$, where $B_3 = \frac{D_s C_s g_3 \Omega^2}{k_B T}$, which is consistent, e.g., with Ref. 9. The reduced PDE is applied to smooth regions of periodic corrugations.[3,9,11] For concentric circular, descending steps of radius r (in 2D), we have $\kappa = 1/r$ and Eq. (12) becomes $\partial_t h = Br^{-1}\partial_r\{(1 + qm)^{-1}[-r^{-1} + \frac{g_3}{g_1} r \partial_r(r^{-1}\partial_r(rm^2))]\}$, where $m = |\partial_r h|$, which is suitable for smooth regions of axisymmetric mounds.[10,12,15]

We next apply separation of variables to Eq. (12) for smooth regions of biperiodic profiles, aiming to unify decay laws in relaxation experiments. Consistent with step simulations in 1D[9] and kinetic Monte Carlo simulations in 2D,[13]

TABLE I. Decay laws for the amplitude $A(t)$ in ADL kinetics. Top row: kinetic-geometric conditions on mobility, Eqs. (8)–(10). Leftmost column: dominant effects in μ, Eq. (11). The constants $\mathcal{C}$, c, and t^* ($t^* > t$) depend on $A(0) = A_0$ and H.

	$\alpha^2 \ll \beta \ll 1$	$\beta \ll \alpha^2 \leq 1$
Step interaction	$A_0 e^{-\mathcal{C} B_3 t}$	$A_0(1 + c B_3 A_0 t)^{-1}$
Line tension	$A_0 \sqrt{1 - t/t^*}$	$A_0(1 - t/t^*)$

both for initial sinusoidal profiles, we set $h(\mathbf{r}, t) \approx A(t)H(\mathbf{r})$ and find $A(t)$. This variable separation, which we call a "scaling ansatz," is satisfied only approximately: additive terms in μ and $\mathbf{M}$ scale differently with A. In μ, Eq. (11), the step line tension (g_1 term) scales with A^0 and the step interaction (g_3 term) scales with A^2; in M_{ij}, Eqs. (8)–(10), the kinetic term $\beta = (1 + q\langle|\nabla h|\rangle)^{-1}$ must be compared to the aspect ratio squared, α^2; $\langle|\nabla h|\rangle \equiv \nu$ is a typical slope.

Here, we do not address the evaluation of $H(\mathbf{r})$, which solves a nonlinear PDE. Because boundary conditions for H at facet edges require feedback from step simulations,[15] a numerical scheme for H within continuum is not currently feasible. By Refs. 9 and 13, the scaling ansatz seems reasonable for long t and initial sinusoidal profiles.

We next focus on ADL kinetics, $\beta \ll 1$, distinguishing four cases. In the first case, (i) step interactions dominate, $|g_3 \nabla \cdot (|\nabla h| \nabla h)| \gg |g_1 \kappa|$ or $\frac{g_3}{g_1} \gg \left(\frac{\alpha}{\nu} \right)^2$ by dimensional analysis for sinusoidal profiles, where $\nu \approx \frac{h_{pv}}{\lambda/2}$ and h_{pv} is the peak-to-valley height variation, and (ii) $\beta < \alpha^2$ so that longitudinal fluxes are considerable. Thus, μ scales with A^2, and the matrix elements of $\mathbf{\Lambda}$ are $\Lambda_{xx} \approx -\frac{(\partial_y h)^2}{|\nabla h|^2}$, $\Lambda_{yy} \approx -\frac{(\partial_x h)^2}{|\nabla h|^2}$, and $\Lambda_{xy} = \Lambda_{yx} \approx \frac{(\partial_x h)(\partial_y h)}{|\nabla h|^2}$, which scale with A^0 as in TDL kinetics. We find $dA/dt \approx -cB_3 A^2$. Hence,

$$A(t) = A_0(1 + cB_3 A_0 t)^{-1}, \quad A_0 := A(0). \tag{13}$$

The constant c [(length)$^{-4}$] depends on H and is thus influenced by facets. Equation (13) suggests an inverse linear decay with time if the (y) adatom flux in the direction of the longer wavelength (λ_y) is significant.

In the second case, (i) step interactions remain dominant and (ii) $\beta > \alpha^2$, so that transverse fluxes prevail. Thus, we obtain $dA/dt = -\mathcal{C} B_3 A$, by which

$$A(t) = A_0 e^{-\mathcal{C} B_3 t}, \tag{14}$$

where $\mathcal{C}$ is influenced by H. The remaining cases for ADL kinetics follow similarly. The results are summarized in Table I. The square-root decay with time when line tension dominates and $\beta > \alpha^2$ is in agreement with Ref. 13.

Our predictions, based on Eq. (12) with ADL kinetics, can be extended to TDL kinetics. The mobility $\mathbf{M}$ then reduces to $\frac{D_s}{k_B T}$. Thus, we obtain Eq. (13) or Eq. (14), regardless of α, for step-interaction- or line-tension-dominated μ.

Next, we compare our predictions with observations on Si(001) (Refs. 3 and 5) and Ag(110).[6] In Si(001), with $\ell \equiv 2D_s/k \gtrsim 1000$ nm[7] and terrace width $\Delta w \lesssim 10$ nm,[3,5,7] $q\langle|\nabla h|\rangle \approx \frac{\ell}{\Delta w} \gtrsim 100$ which suggests ADL kinetics. We find

decay laws comparing (i) the kinetic factor β, $\beta \approx \frac{\Delta w}{\ell} \lesssim 0.01$, with the aspect ratio squared, $\alpha^2 \approx \left(\frac{\lambda_x}{\lambda_y}\right)^2$, and (ii) the relative strength of step interactions, $\frac{g_3}{g_1}$, with $\left(\frac{\alpha}{\nu}\right)^2$. In Ref. [3], $\alpha \approx 10^{-3}$ and thus $\beta \gg \alpha^2$. Also, $\nu \approx 1/30$ and $\frac{g_3}{g_1} > 1$,[21] and thus $\frac{g_3}{g_1} \gg \left(\frac{\alpha}{\nu}\right)^2$. Equation (14) follows, in agreement with Ref. [3]. In Ref. [5], $\alpha \gtrsim 10^{-1}$, $\nu \approx 1/15$, and $\frac{g_3}{g_1} \approx 100$.[21] So, $\beta < \alpha^2$ and $\frac{g_3}{g_1} > \left(\frac{\alpha}{\nu}\right)^2$. Equation (13) follows, in agreement with Ref. [5].

Note that Si(001) may have properties not entirely consistent with Eq. (12), e.g., terrace diffusion is anisotropic and step interactions can deviate from (4).[22] Although the terrace anisotropy modifies **M**, it does not change the scalings with time.[23] Further, the assumed dipole interactions can dominate on Si(001) when terraces are sufficiently narrow, e.g., when double steps form.[22]

We now discuss observations on Ag(110) (Ref. [6]) where step interactions are mainly entropic.[2,24] By $\beta < 10^{-36}$ and $\alpha \approx 1/15$,[25] we have $\beta < \alpha^2$. We estimate $\frac{g_3}{g_1}$ by $g_1 = \frac{\epsilon_k}{aa_0} - \frac{k_B T}{aa_0}\ln\left(\coth\frac{\epsilon_k}{2k_B T}\right)$ and $g_3 \approx \frac{\pi^2 a_0 k_B T}{2a^3}\left[\sinh\left(\frac{\epsilon_k}{2k_B T}\right)\right]^{-2}$, where ϵ_k is the kink formation energy, $0.04 \text{ eV} \lesssim \epsilon_k \lesssim 0.1 \text{ eV}$,[2,26] $a = 1.4$ Å, $a_0 \approx 4$ Å, and $T = 210$ K; thus, $\frac{2}{17} \lesssim \frac{g_3}{g_1} \lesssim 1$. With $\nu \approx 2/25$,[6,27] $\frac{g_3}{g_1} = O\left(\frac{\alpha^2}{\nu^2}\right)$; thus, our criterion for step energetics appears inconclusive for scaling. A possible reason is the terrace anisotropy of Ag(110), which may modify the numerical values of requisite parameters. Further study of the dynamics with reliable boundary conditions at facets is indicated.

Our work forms a basis for a general approach to morphological evolution below roughening. Extensions in 2D include the Ehrlich-Schwoebel (ES) barrier,[28] long-range step interactions, step-edge diffusion, anisotropy of step stiffness, and material deposition. Inclusion of the ES barrier[28] with rates k_u and k_d amounts effectively to $k = 2(1/k_u + 1/k_d)^{-1}$ in Eq. (12).[16] Step-edge diffusion contributes to longitudinal fluxes but may not be important for Si(001).[2]

Connecting predictions of Eq. (12) to actual experimental situations has yet to be explored. Our scaling ansatz should be tested for realistic initial profiles. Despite couplings caused by nonlinearities,[14] our scaling should be valid for a range of prevailing wavelengths.[5,6,14] Other predictions of our approach include crossovers from exponential to inverse linear profile decay via aspect-ratio changes of the surface shape. Our work should stimulate further studies and relaxation experiments on crystal surfaces below roughening.

[1] W. K. Burton, N. Cabrera, and F. C. Frank, Philos. Trans. R. Soc. London, Ser. A **243**, 299 (1951).

[2] H.-C. Jeong and E. D. Williams, Surf. Sci. Rep. **34**, 171 (1999).

[3] M. E. Keefe, C. C. Umbach, and J. M. Blakely, J. Phys. Chem. Solids **55**, 965 (1994).

[4] J. Blakely, C. Umbach, and S. Tanaka, in *Dynamics of Crystal Surfaces and Interfaces*, edited by P. M. Duxbury and T. J. Pence (Plenum, New York, 1997), p. 23.

[5] J. Erlebacher, M. J. Aziz, E. Chason, M. B. Sinclair, and J. A. Floro, Phys. Rev. Lett. **84**, 5800 (2000).

[6] L. Pedemonte, G. Bracco, C. Boragno, F. B. de Mongeot, and U. Valbusa, Phys. Rev. B **68**, 115431 (2003).

[7] N. Israeli and D. Kandel, Phys. Rev. Lett. **88**, 169601 (2002).

[8] J. Erlebacher, M. J. Aziz, E. Chason, M. B. Sinclair, and J. A. Floro, Phys. Rev. Lett. **88**, 169602 (2002).

[9] N. Israeli and D. Kandel, Phys. Rev. B **62**, 13707 (2000).

[10] N. Israeli and D. Kandel, Phys. Rev. Lett. **80**, 3300 (1998); Phys. Rev. B **60**, 5946 (1999).

[11] A. Rettori and J. Villain, J. Phys. (France) **49**, 257 (1988); M. Ozdemir and A. Zangwill, Phys. Rev. B **42**, 5013 (1990); H. Spohn, J. Phys. I **3**, 69 (1993); H. P. Bonzel and W. W. Mullins, Surf. Sci. **350**, 285 (1996); V. B. Shenoy and L. B. Freund, J. Mech. Phys. Solids **50**, 1817 (2002).

[12] D. Margetis, M. J. Aziz, and H. A. Stone, Phys. Rev. B **71**, 165432 (2005).

[13] V. B. Shenoy, A. Ramasubramaniam, H. Ramanarayan, D. T. Tambe, W. L. Chan, and E. Chason, Phys. Rev. Lett. **92**, 256101 (2004).

[14] W. L. Chan, A. Ramasubramaniam, V. B. Shenoy, and E. Chason, Phys. Rev. B **70**, 245403 (2004).

[15] D. Margetis, P.-W. Fok, M. J. Aziz, and H. A. Stone, Phys. Rev. Lett. **97**, 096102 (2006).

[16] D. Margetis and R. V. Kohn, Multiscale Model. Simul. **5**, 729 (2006).

[17] A. Natori and R. W. Godby, Phys. Rev. B **47**, 15816 (1993).

[18] S. Paulin, F. Gillet, O. Pierre-Louis, and C. Misbah, Phys. Rev. Lett. **86**, 5538 (2001).

[19] G. Danker, O. Pierre-Louis, K. Kassner, and C. Misbah, Phys. Rev. Lett. **93**, 185504 (2004).

[20] V. I. Marchenko and A. Ya. Parshin, Sov. Phys. JETP **52**, 129 (1980).

[21] T. W. Poon, S. Yip, P. S. Ho, and F. F. Abraham, Phys. Rev. B **45**, 3521 (1992); H. J. W. Zandvliet, Rev. Mod. Phys. **72**, 593 (2000).

[22] B. S. Swartzentruber, N. Kitamura, M. G. Lagally, and M. B. Webb, Phys. Rev. B **47**, 13432 (1993); T. W. Poon, S. Yip, P. S. Ho, and F. F. Abraham, Phys. Rev. Lett. **65**, 2161 (1990).

[23] J. Quah and D. Margetis (unpublished).

[24] W. W. Pai, J. S. Ozcomert, N. C. Bartelt, T. L. Einstein, and J. E. Reutt-Robey, Surf. Sci. **307-309**, 747 (1994).

[25] F. Buatier de Mongeot (private communication).

[26] L. Vitos, H. L. Skriver, and J. Kollár, Surf. Sci. **425**, 212 (1999).

[27] U. Valbusa, C. Boragno, and F. Buatier de Mongeot, J. Phys.: Condens. Matter **14**, 8153 (2002).

[28] G. Ehrlich and F. Hudda, J. Chem. Phys. **44**, 1039 (1966); R. L. Schwoebel and E. J. Shipsey, J. Appl. Phys. **37**, 3682 (1966).